Available online at www.sciencedirect.com
ScienceDirect
Optics Communications 274 (2007) 260–267
OPTICS COMMUNICATIONS
www.elsevier.com/locate/optcom

Time-resolved fluorescence polarization anisotropy and optical imaging of Cybesin in cancerous and normal prostate tissues

Y. Pu [a], W.B. Wang [b], S. Achilefu [c], B.B. Das [b], G.C. Tang [b], V. Sriramoju [b], R.R. Alfano [b,*]

[a] *Institute for Ultrafast Spectroscopy and Lasers and New York State Center for Advanced Technology for Ultrafast Photonic Materials and applications, Department of Electrical Engineering, The City College of the City University of New York, Convent Avenue at 138th Street, New York, NY 10031, United States*

[b] *Institute for Ultrafast Spectropscopy and Lasers, and New York State Center for Advanced Technology for Ultrafast Photonic Materials and Applications, Department of Physics, The City College of the City University of New York, Convent Avenue at 138th Street, New York, NY 10031, United States*

[c] *Washington University School of Medicine, 4525 Scott Avenue, St. Louis, MO 63110, United States*

Received 12 May 2006; received in revised form 15 January 2007; accepted 22 January 2007

Abstract

Time-resolved polarization-dependent fluorescence of Cybesin in solution and in cancerous and normal prostate tissues were measured. The polarization preservation property of Cybesin in tissue was observed. The fluorescence intensity emitted from a Cybesin-stained cancerous tissue area was found to be much stronger than that from a Cybesin-stained normal tissue area indicating that cancerous prostate tissue takes-up more Cybesin than normal tissue. The polarization anisotropy of Cybesin contained in cancerous prostate tissue was found to be larger than that of Cybesin in normal prostate tissue indicating that a larger degree of polarization was preserved in the Cybesin-stained cancerous tissue due to structures. A static anisotropy component from the emission of cell-bonded Cybesin molecules in tissue and a time-dependent anisotropy component from the emission of un-bonded Cybesin molecules were determined and discussed. The static anisotropy value of Cybesin in stained cancerous tissue was found to be much larger than that in stained normal tissue. The fluorescence polarization difference imaging technique based on the polarization preservation of Cybesin was used to enhance the image contrast between cancerous and normal prostate tissue areas.

Keywords: Prostate cancer receptor-targeted contrast agent; Time-resolved fluorescence polarization kinetics; Polarization anisotropy; Polarization preservation; Fluorescence polarization difference imaging

1. Introduction

Prostate cancer has a high incidence and mortality rate in men. Every year, nearly 180,000 new prostate cancer cases are diagnosed, and about 37,000 deaths are caused by prostate cancer in the US [1]. Common methods for prostate cancer diagnosis are the prostate specific antigen (PSA) test, digital rectal examination (DRE), trans-rectal ultrasound (TRUS) imaging and biopsy [2]. Among these conventional techniques, PSA and DRE have limited accuracy, ultrasound imaging has limited contrast and resolution, and biopsy is invasive. In the last two decades, optical spectroscopy [3] and imaging [4] have been rapidly gaining acceptance as important diagnostic tools in the imaging of cancerous tissue due to their high sensitivity and resolution [4]. As newer optical methods, fluorescent spectroscopy and imaging have received lots of attention. These methods can apply intrinsic or extrinsic fluorophore. The use of intrinsic fluorescent chromophores to differentiate the optical properties of diseased and healthy human tissues is mostly limited by their ultraviolet pumping

* Corresponding author. Tel.: +1 212 650 5531; fax: +1 212 650 5530.
E-mail address: alfano@sci.ccny.cuny.edu (R.R. Alfano).

0030-4018/$ - see front matter © 2007 Elsevier B.V. All rights reserved.
doi:10.1016/j.optcom.2007.01.078

wavelengths [5], which are not in the "optical window" of tissue [6]. Fluorescing optical contrast agents were introduced to increase sensitivity and specificity using extrinsic fluorescence for tumor detection to enhance differentiating cancer from normal tissue [7,8].

Previous works has shown that cancer cells will overexpress certain receptors, and increase the uptake of the corresponding ligands. Conjugation of a fluorophore to those ligands can give high fluorescent contrast for tumor cells versus the normal cells. Achilefu et al. [9] have developed a small indocyanine green (ICG)-derivative dye-peptide, cypate-bombesin peptide analogue conjugate (Cybesin), to target the over-expressed bombesin receptors on pancreas tumors in an animal model [9]. The study of receptor specificity on tumor has indicated that bombesin belongs to a family of brain-gut peptides that play an important role in cancer development [10]. It was also observed several years ago that human primary tumors can synthesize bombesin [10], and the bombesin receptor can also be over-expressed on the membranes of human prostate cancer cells [10]. These results motivated us to apply Cybesin to human prostate cancer detection. Cybesin was successfully applied in detecting human prostate cancer in vitro by using an optical fluorescence imaging technique [11].

The time-resolved polarization properties of fluorescence from ICG and their application for polarization imaging have been investigated [12]. The results show that the temporal intensity profiles of light emitted at polarized directions parallel ($\|$) and perpendicular ($\perp$) to the polarization direction of a linearly polarized excitation are different [12]. The polarization preservation property of ICG fluorescence makes it possible for it to be used as a polarization contrast agent to enhance the image quality [12,13].

In this study, the time-resolved fluorescence polarization profiles of Cybesin in solution and in Cybesin-stained cancerous and normal prostate tissues were obtained. The measured fluorescence intensities and the resultant fluorescence polarization anisotropies can be explained by the preferential uptake of Cybesin in human cancerous prostate tissue, and show the polarization preservation property of Cybesin in tissue.

The experimental data obtained from a Cybesin solution was fitted using a time-dependent fluorescence depolarization model [14,15]. The resultant parameters for Cybesin solution compared to those for Cybesin-stained tissue are useful in understanding the effect of the rotational degree of freedom of Cybesin in tissue. An empirical model was developed to describe the time-resolved fluorescence kinetics and polarization anisotropy of Cybesin in human prostate tissue. Prostate samples consisting of a small piece of normal prostate tissue and a small piece of prostate cancer tissue stained with Cybesin were imaged. The image contrast between cancerous and normal areas, and the spatial resolution of fluorescence polarization difference imaging were an improvement over the conventional optical imaging approach.

2. Model of fluorescence depolarization

The fluorescence depolarization technique is widely used as a probe for rotational motion of molecules in solution. A fluorescent molecule, absorbing light at time t, can undergo a rotation before emitting light at some later time. This rotation affects the angle between the polarization vectors of absorption and emission, and is most sensitively investigated when linearly polarized light is used to excite the molecule and a particular polarization component of emission is detected [15]. The fluorescence depolarization property is usually described by the time-resolved fluorescence polarization anisotropy which is defined as [14,15]:

$$r(t) = \frac{I_{\|}(t) - I_{\perp}(t)}{I_{\|}(t) + 2I_{\perp}(t)} \tag{1}$$

where $I_{\|}(t)$ and $I_{\perp}(t)$ are the emission intensities of the fluorescent polarization components which are parallel and perpendicular to that of the excited light, respectively [14,15]. The reorientation of a fluorescent dye in solvent will result in the decay behavior of $r(t)$. In a simple possible case where the Cybesin molecule undergoes Brownian rotation as an Einstein sphere, the time-resolved fluorescence kinetics and polarization anisotropy of a Cybesin solution can be modeled using the equation [14,15]:

$$r(t) = r(0)\exp\left(-\frac{t}{\tau_{\text{rot}}}\right) \tag{2}$$

where the rotation time τ_{rot} can be expressed in terms of the diffusion coefficient (D), or the solvent viscosity (η) and the molecular radius (a) by:

$$\tau_{\text{rot}} = (6D)^{-1} = \frac{4\pi\eta a^3}{3kT} \tag{3}$$

where k is the Boltzmann constant and T is the absolute temperature of the solvent [15]. The emission anisotropy at $t = 0$ is given by:

$$r(0) = \left(\frac{2\langle P_2^2\rangle + \langle P_2\rangle}{1 + 2\langle P_2\rangle}\right) P_2(\cos\delta) \tag{4}$$

where δ is the angle between the absorption and emission dipoles, and $\langle P_2\rangle$ is the expectation value of the second order Legendre polynomial for the distribution function $f(\theta)$ of dipoles [16,17], which is given by:

$$\langle P_2\rangle \equiv \langle P_2(\cos\theta)\rangle = \int_0^{\pi} \sin\theta\, \mathrm{d}\theta f(\theta) P_2(\cos\theta) \tag{5}$$

where θ is the angle between the long axis of the molecule and the major symmetry axis of the system [15,16]. For the case of a Cybesin solution in which the viscosity is low, the random distribution function $f(\theta) = 1/2$ is taken. Using this function and the above equations, the theoretical value of $r(0)$ for a Cybesin solution was calculated to be 0.4.

The value of $r(0)$ for the fluorescence anisotropy of a dye depends on the viscosity of the solvent [17,18]. Above a critical value of the viscosity of ~3000 P, a normalized orientational distribution function $f(\theta) = 3/2\cos^2\theta$ was used

as a model for fluorescent molecules [17,18]. By taking this distribution function and using Eqs. (4) and (5), a calculated value of $r(0) = 0.1039$ was obtained. The fluorescence anisotropies of Malachite green in glycerol in the viscosity range of 1–60,000 P have been measured [17]. Results indicate that for viscosities greater than 3000 P, the experimental value $r(0)$ of Malachite green in glycerol was found to be $\sim 0.11 \pm 0.01$ [17,18], which was in fair agreement with the calculated value obtained by the normalized orientational distribution.

Biological living tissues may mimic the behavior of viscous liquids [19,20]. It is expected to have ordered structure. The viscosities of biological tissues were reported to be much higher than 3000 P [20,21]. If the case of Cybesin in prostate tissue is considered as a fluorescent dye in a "very high viscosity liquid", the anisotropy $r(0)$ is expected to be in the range between ~ 0.10 and ~ 0.12.

3. Experimental method

The experimental arrangement of the time-resolved fluorescence measurements for the Cybesin solution and for Cybesin-stained cancerous and normal prostate tissues is schematically shown in Fig. 1. Optical pulses of 130 fs at 800 nm with a repetition rate of 82 MHz from a Coherent Mira 900 Mode-locked Ti:Sapphire laser were used to pump the samples. The fluorescence was collected by a large diameter lens (L_2) with a focal length of 5 cm and directed onto a synchroscan streak camera with temporal resolution of 10 ps. A long pass filter (LP) was used to block the illuminating light so that only the emission from the samples was detected. Polarizer P_1 was used to ensure the linear polarization of the input laser pulses and P_2 was used as an analyzer. The polarization of P_1 was rotated between 0° and 90° with respect to that of P_2 to record the intensity profiles of the parallel and perpendicular polarization components of the fluorescence. The temporal profiles of fluorescence recorded by a silicon intensified target (SIT)

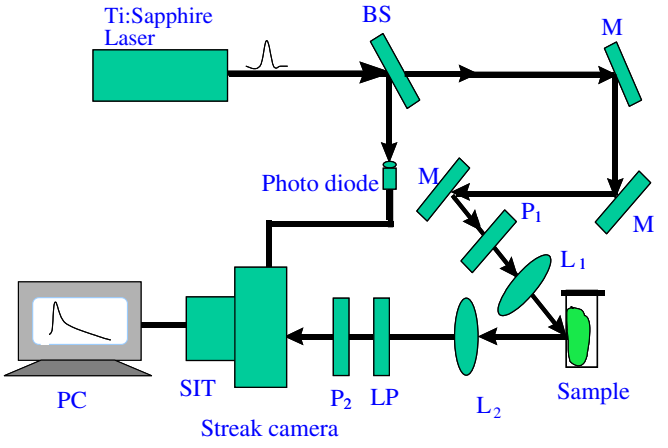

Fig. 1. Schematic diagram of the experimental set up used for time-resolved fluorescence measurements, where P_1, P_2: polarizers; M: mirrors; BS: beam splitter; LP: long pass filter; L: lenses; SIT: silicon intensified target.

vidicon camera were analyzed to obtain the temporal profiles and polarization dynamics of the fluorescence.

The Cybesin used for the time-resolved fluorescence study was solvated in 20% aqueous dimethyl sulfoxide (DMSO). Cybesin was prepared by Achilefu's group at the Washington University School of Medicine. The molecular structure, synthesis and the absorption and fluorescence spectra of the Cybesin agent have been reported elsewhere [9,11]. The Cybesin agent is mainly composed of ICG and the bombesin receptor ligand, which delivers the contrast agent to the corresponding receptor presented in the tumor [9]. The absorption band of Cybesin ranges from 680 nm to 830 nm with a strong peak at 792 nm and a shoulder peak at 720 nm. The fluorescence spectrum of Cybesin appears between 800 nm and 950 nm with a main peak at 825 nm and a weak peak at 925 nm [11].

Six (6) in vitro prostate cancer-and-normal tissue samples obtained from the National Disease Research Interchange (NDRI), the Cooperation Human Tissue Network (CHTN) and the Hackensack University Medical Center (HUMC) were used for the time-resolved fluorescence and optical imaging measurements under IRB approvals at the City College of New York. Samples were not chemically treated and they were not frozen prior to our measurements. The cancerous and normal prostate tissues used for the temporal fluorescence measurements were cut into $\sim 2 \times \sim 1 \times \sim 0.5$ cm (length × width × thickness) pieces, and were soaked in the same Cybesin–DMSO (20% aqueous Dimethyl Sulfoxide) solution with a Cybesin concentration of $\sim 3.2 \times 10^{-6}$ M for the same period of time. Then the samples were put into sodium phosphate buffer (Sigma–Aldrich) to wash off and consequently reduce the amount of unbound Cybesin. All the measurements and processes were performed at room temperature.

The spectral polarization imaging set up used for imaging Cybesin-stained cancerous and normal prostate tissue has been described elsewhere [11]. Light from a white light source is used to illuminate the prostate tissue samples with average power of about 50 μW/cm^2. The wavelengths of the pump and detection are selected by wide band pass filters with central wavelengths varying from 550 nm to 900 nm with FWHM = 40 nm. A CCD camera records images formed by light emitted from the samples. The spatial resolution of the spectral polarization imaging system is 20 μm. Polarizers were used to obtain parallel and perpendicular images relative to the polarization direction of the illuminating light.

A typical cancerous-normal prostate tissue sample used for the imaging measurements consists of a small piece of prostate cancer tissue and a small piece of normal prostate tissue. They were treated with the Cybesin agent in the same way as described above for the temporal fluorescence measurements. The stained normal and cancer tissues were then sandwiched between large pieces of normal prostate tissue.

Histopathological measurements were performed on the cancerous and normal prostate tissue samples to confirm the presence of the tumor cells in the cancerous prostate tissue samples. The prostate tissues from which the stained

normal and cancerous tissue pieces were taken for the imaging measurements were cut into a number of thin slides with a thickness of 250 μm for microscopy tissue section study. The microscope images of the histological slices were taken using a digital electro-microscope (Mel Sobel Microscopes Ltd.). The different microstructures of the normal and cancerous prostate tissues corresponding to the typical normal and cancerous microstructures were observed from their microscope images (×40), and the presence of the tumor cells in the cancerous tissue pieces was identified [11]. The histopathological results were compared with the results obtained from the optical imaging using the contrast agent Cybesin.

4. Experimental results and discussion

4.1. Time-resolved fluorescence kinetics and polarization anisotropy of Cybesin in 20% aqueous DMSO

The measured temporal profiles of the fluorescence emitted from Cybesin for polarizations parallel and perpendicular to the polarization direction of the excitation at 800 nm are shown in Fig. 2a. The thick- and thin-line profiles are the parallel and the perpendicular components $I_{\parallel}(t)$ and $I_{\perp}(t)$, respectively. The main difference between these two components is that $I_{\parallel}$ is greater than $I_{\perp}$ for all of the decay times. In particular, at the peak position ($t = 0$), the parallel component $I_{\parallel}(0)$ is almost three (3) times stronger than that of the perpendicular one $I_{\perp}(0)$. This indicates the polarization preservation nature of Cybesin.

Using Eq. (1), the calculated temporal profile of the polarization anisotropy $r(t)$ of Cybesin in solution is shown as a thin line in Fig. 2b. The $r(0)$ obtained from Fig. 2b is 0.39, which is very close to the theoretical value of 0.4. This indicates that the transition dipole moments of Cybesin molecules in solution are randomly oriented and that the depolarization effects of Cybesin in 20% DMSO solvent can be confined to molecular rotations and to the trivial effect of initial randomness [14]. The polarization anisotropy peak value $r(0)$ and the rotation time τ_{rot} of Cybesin in solution can be obtained using Eq. (2) to fit the experimental data of $r(t)$ in Fig. 2b. The fitting curve calculated using the experimental data of $r(t)$ and Eq. (2) is shown by the thick line in Fig. 2b. The fitting results show $r(0) = 0.389 \pm 0.028$ and $\tau_{rot} = 359 \pm 19$ ps.

4.2. Time-resolved fluorescence kinetics and polarization anisotropy of Cybesin contained in stained cancerous and normal prostate tissues

For the time-resolved fluorescence measurements of Cybesin-stained cancerous and normal tissues, six (6) cancerous tissue and six (6) normal tissue samples were used. The average time-resolved fluorescence intensity profiles for these six (6) samples of the cancerous and normal prostate tissues stained with Cybesin are displayed in Fig. 3a. The thick-solid- and thick-dash-line profiles are the parallel

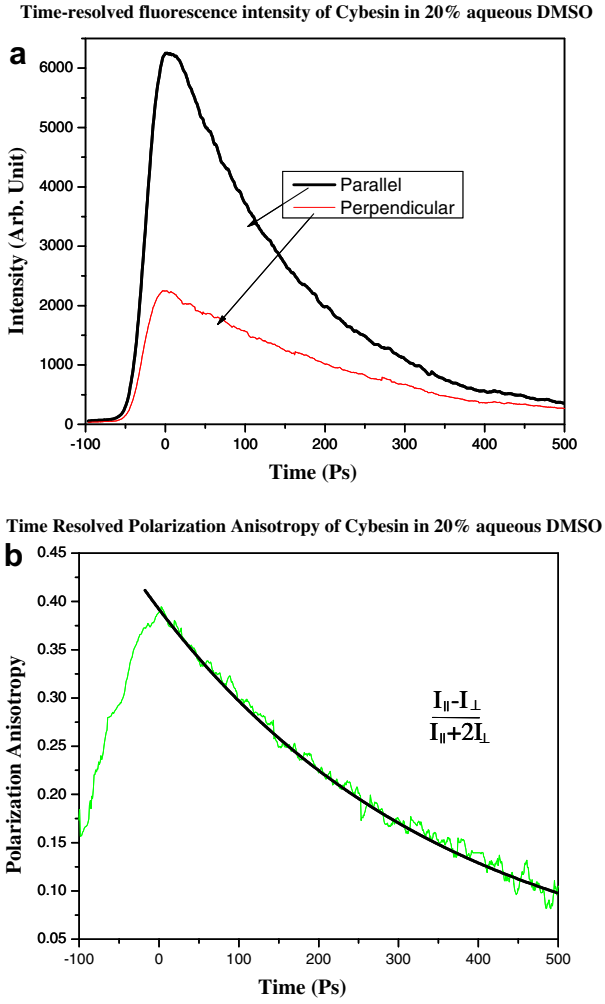

Fig. 2. Temporal polarization profiles and polarization anisotropy of light emitted from Cybesin in 20% aqueous DMSO with linear polarized 800 nm laser illumination. (a) Profiles of the time-resolved emission components having a polarization direction parallel (thick line) and perpendicular (thin line) to the polarization direction of the exciting light. (b) Time-dependent polarization anisotropy (thin line) calculated using the measured data shown in (a) and Eq. (1) in the text, and the fitting curve (thick line) calculated using Eq. (2) and the data of $r(t)$ in (b).

and perpendicular components emitted from stained cancerous tissue, respectively. The thin-solid- and thin-dash-line profiles display the parallel and perpendicular components emitted from stained normal tissue, respectively.

The most obvious feature of Fig. 3a is that the emission intensities from stained cancerous tissue are larger than those of stained normal tissue for the life time of Cybesin emission. The emission peak of Cybesin-stained cancerous tissue is much greater than that of stained normal tissue. For example, for the parallel polarization configuration, the ratio of peak fluorescence intensity of Cybesin-stained cancerous tissue to that of the normal is found to be ~3.63, while for the perpendicular configuration, the ratio is ~3.23. These indicate that cancerous prostate tissue takes-up more Cybesin than normal tissue does.

Another important feature from Fig. 3a is that $I_{\parallel}$ is greater than $I_{\perp}$ for both cancerous and normal tissue for

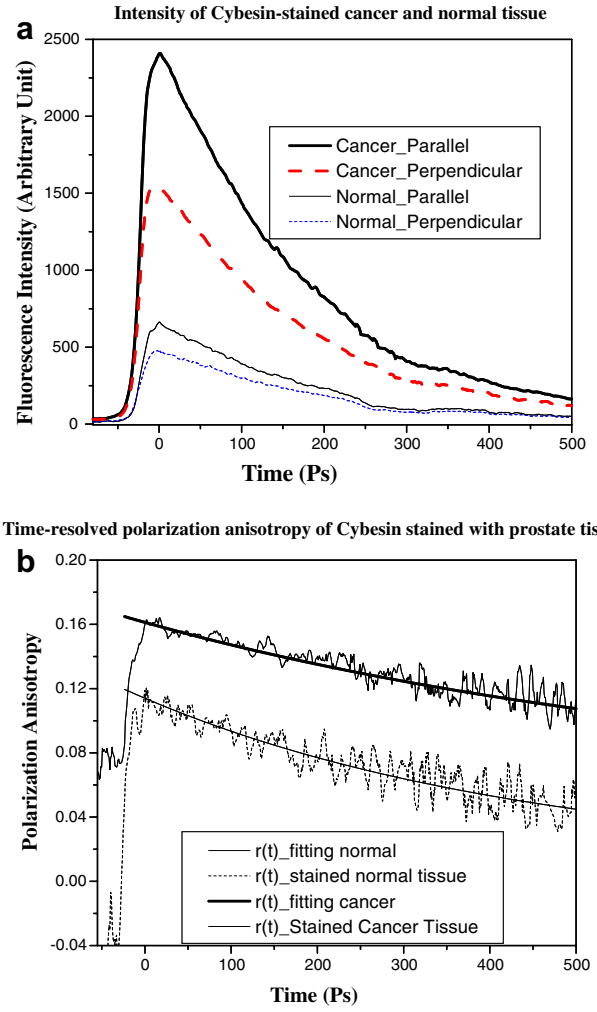

Fig. 3. (a) The time-resolved fluorescence intensity of light emitted from Cybesin-stained cancerous and normal prostate tissues for linearly polarized 800 nm laser illumination. The thick-solid- and thick-dash-line profiles are the parallel and perpendicular components emitted from stained cancerous tissue, respectively. The thin-solid- and thin-dash-line profiles display the parallel and perpendicular components emitted from stained normal tissue, respectively. (b) Time-dependent polarization anisotropy calculated using Eq. (1) shown in the text and the measured data shown in (a). The thin-solid and thin-dash line profiles indicate the $r(t)$ for stained cancerous and normal prostate tissues, respectively. The fitting curves for Cybesin in cancer tissue (thick solid line) and Cybesin in normal tissue (thin solid line) were calculated using Eq. (6) and the corresponding polarization anisotropy shown in (b).

all of the decay times. At the peak position, $I_{\parallel}^{\text{cancer}}(0)$ is $\sim$1.57 times stronger than $I_{\perp}^{\text{cancer}}(0)$, and the ratio of $I_{\parallel}^{\text{normal}}(0)$ to $I_{\perp}^{\text{normal}}(0)$ is $\sim$1.40. This indicates that the fluorescence emitted from Cybesin-stained cancerous and normal prostate tissue still show the polarization preservation property, although the ratio of $I_{\parallel}$ to $I_{\perp}$ dropped compared to Cybesin solution. Using the measured values of $I_{\parallel}(t)$ and $I_{\perp}(t)$ shown in Fig. 3a, the temporal profiles of the polarization anisotropy $r(t)$ of the fluorescence emitted from Cybesin in stained cancerous (thin-solid line) and normal (thin-dash line) prostate tissue are calculated using Eq. (1) and displayed in Fig. 3b. This shows the valuable feature that the polarization anisotropy of stained cancerous tissue is always larger than that of normal tissue within the emission life-time of Cybesin.

The interesting features of the $r(t)$ curves shown in Fig. 3b are: (1) the profiles of Cybesin-stained tissue show a flatter decay in comparison with Cybesin solution; and (2) the values of the polarization anisotropy of Cybesin in the stained cancerous tissue are always larger than that of the stained normal tissue for all the decay times. The peak intensity values of $r(0)$ for cancerous and normal tissues were found as: $r(0)^{\text{cancer}} = 0.163 \pm 0.014$ and $r(0)^{\text{normal}} = 0.120 \pm 0.012$. These results indicate that the Cybesin-stained cancerous tissue shows a better polarization preservation property than the Cybesin-stained normal prostate tissue.

The experimental values of $r(0)$ for Cybesin in tissue are larger than that we would have expected since $r(0)$ should be around 0.11 ± 0.01 for solutions of viscosity greater than 3000 P using the normalized orientational distribution function [17,18]. To understand this, a model describing two types of Cybesin molecules in Cybesin-stained prostate tissue and their contributions to fluorescence polarization anisotropy is developed. Fig. 4 shows a schematic diagram of the model illustrating the cell-bonding mechanism and reorientation of Cybesin molecules in prostate tissue. The time-resolved fluorescence polarization anisotropy $r(t)$ of Cybesin in stained human prostate tissue can be considered having two components:

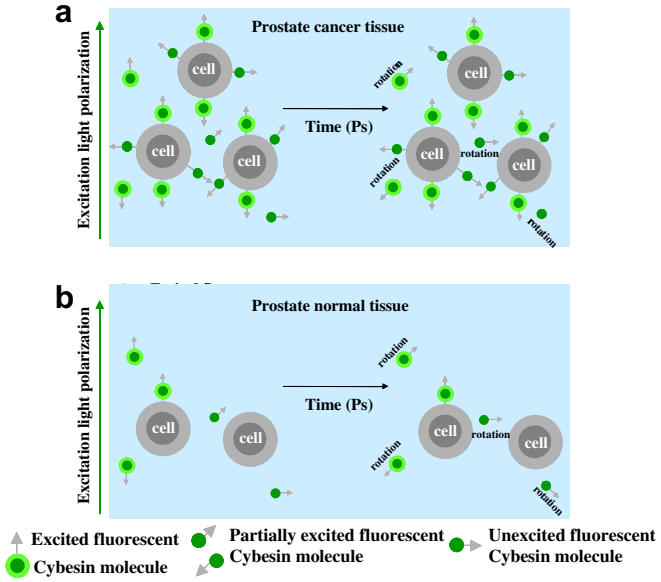

Fig. 4. The schematic diagrams of a physical model of the cell-bonding mechanism and reorientation of Cybesin in stained (a) cancerous tissue which has a higher cell density and more cell-bonded Cybesin, and (b) normal tissue which has a lower cell density and less cell-bonded Cybesin. Cybesin molecules with their absorption transition vectors (arrows) aligned parallel to linearly polarized pump light (for example: vertical), and those having a parallel component of other-orientated transition vectors are excited. For free Cybesin molecules, the rapid rotations contribute fluorescence depolarization. In contrast, Cybesin conjugated to prostate cells shows a static anisotropy component.

(1) a static anisotropy component formed by the emission of the cell-bonded Cybesin molecules without rotation; and (2) a time-dependent anisotropy component formed by the emission of the un-bonded Cybesin molecules (with rotation) in the body liquid of prostate tissue. Under these assumptions, the temporal fluorescence polarization anisotropy $r(t)$ of Cybesin in stained human prostate tissues can be expressed as:

$$r(t) = r_1 + r_0 \exp\left(-\frac{t}{\tau_{\text{rot}}}\right) \tag{6}$$

where $r_0 \exp\left(-\frac{t}{\tau_{\text{rot}}}\right)$ is the time-dependent portion of the polarization anisotropy induced by the "rotation-free" Cybesin molecules in the liquid of prostate tissue, τ_{rot} is the rotation time of the "free" Cybesin in prostate tissue, r_0 is the peak value of the polarization anisotropy of the "free" Cybesin molecules, and r_1 is the static portion of the polarization anisotropy induced by the cell-bonded Cybesin molecules in prostate tissue.

These assumptions can be understood because the weight of tissue cells is much larger than that of Cybesin molecules, and consequently the tissue cells are too huge to rotate. The emission from the cell-bonded Cybesin molecules without rotation will contribute to the static component r_1. The rotation of the free Cybesin molecules will contribute to r_0 and the decay rate of $r(t)$.

The three parameters of τ_{rot}, r_0 and r_1 can be obtained by fitting the experimental data of $r(t)$ shown in Fig. 3b using Eq. (6).

The fitting curves for Cybesin-stained cancer (thick-solid line) and normal (thin-solid line) prostate tissues are shown in Fig. 3b. The results indicate $r_0 = 0.105 \pm 0.010$, $\tau_{\text{rot}} = 700 \pm 150$ ps and $r_1 = 0.056 \pm 0.010$ for Cybesin-stained cancerous prostate tissue; and $r_0 = 0.103 \pm 0.010$, $\tau_{\text{rot}} = 450 \pm 120$ ps and $r_1 = 0.011 \pm 0.003$ for Cybesin-stained normal tissue.

The fitting results indicate $r_1^{\text{cancer}} > r_1^{\text{normal}}$. This can be understood because the perpendicular component of the fluorescence emitted from the cell-bonded Cybesin molecules is mainly contributed by the photons undergoing multiple scattering [12]. Since the excitation wavelength of 800 nm is close to the strong absorption peak of Cybesin [11], and cancerous prostate tissue takes up more Cybesin than the normal, the stained cancerous tissue areas will absorb much more photons than the stained normal tissue areas [11]. Thus photons from same excitation source should go through deeper in normal prostate tissue than cancerous tissue. As a result, the fluorescence from normal prostate tissue area comes from the Cybesin molecules embedded in deeper tissue layer than that in the cancerous prostate tissue area. The light emitted from stained cancerous tissue areas undergoes less multiple scattering than that from the stained normal tissue, thus the polarization degree and r_1 value of the stained cancerous tissue area is much larger than that of the stained normal tissue area.

The fitting results also show $\tau_{\text{rot}}^{\text{cancer}} > \tau_{\text{rot}}^{\text{normal}}$. The larger decay time of free Cybesin molecules in cancerous prostate tissue indicate the higher local viscosity of cancerous prostate tissue. This can be explained because cancerous prostate tissue has a higher cell density [22], so the rotating molecules have less "free" space.

4.3. Optical imaging

The polarization preservation property of Cybesin in prostate tissues can be used to enhance the imaging contrast between cancerous and normal tissue areas. In the imaging measurements, a small piece of cancerous prostate tissue and a small piece of normal prostate tissue stained with Cybesin and sandwiched between large pieces of normal prostate tissue were investigated. The polarized fluorescence images of a Cybesin-stained cancerous-and-normal prostate tissue sample recorded at $\lambda_{\text{pump}} = 750$ nm and $\lambda_{\text{detection}} = 850$ nm are shown in Fig. 5. Fig. 5a displays the image recorded when the polarization direction of detection is parallel ($\parallel$) to that of the illuminating beam. Fig. 5b displays the image recorded when the polarization direction of detection is perpendicular ($\perp$) to that of the illuminating beam. Fig. 5c displays the difference image obtained by subtracting the perpendicular image (Fig. 5b) from the parallel image (Fig. 5a). Fig. 5d–f shows the digital spatial cross-section intensity distributions of the images shown in Fig. 5a–c, respectively.

It can be seen from the images that the cancerous tissue area is much brighter than that of the normal tissue area. Using the digital data shown in Fig. 5d and e, the ratio of imaging intensity of cancerous to normal areas is found to be ~3.05 under parallel polarization, and ~2.96 for the perpendicular configuration. These are in good agreement with that obtained from the time-resolved fluorescence measurements. In comparison with the histopathological microscope imaging results, the correspondence of the brighter area in optical images and the cancerous microstructures in the histopathological images indicates that cancerous prostate tissue takes-up more Cybesin than the normal prostate tissue does.

The other salient feature is that the relative contrast of cancerous to normal areas in the polarization difference image shown in Fig. 5c is obviously higher than those in the individual polarization images shown in Fig. 5a and b. The contrasts (C) of the cancerous area to the normal area for all of the images shown in Fig. 5 were calculated using

$$C = \frac{I_{\text{c}} - I_{\text{n}}}{I_{\text{c}} + I_{\text{n}}} \tag{7}$$

where I_{c} and I_{n} are the local maximum intensities of the dyed cancerous and normal tissue areas, respectively. Using the digital data shown in Fig. 5d–f, the contrasts for these parallel, perpendicular and polarization difference images are calculated to be 0.28, 0.26 and 0.45, respectively.

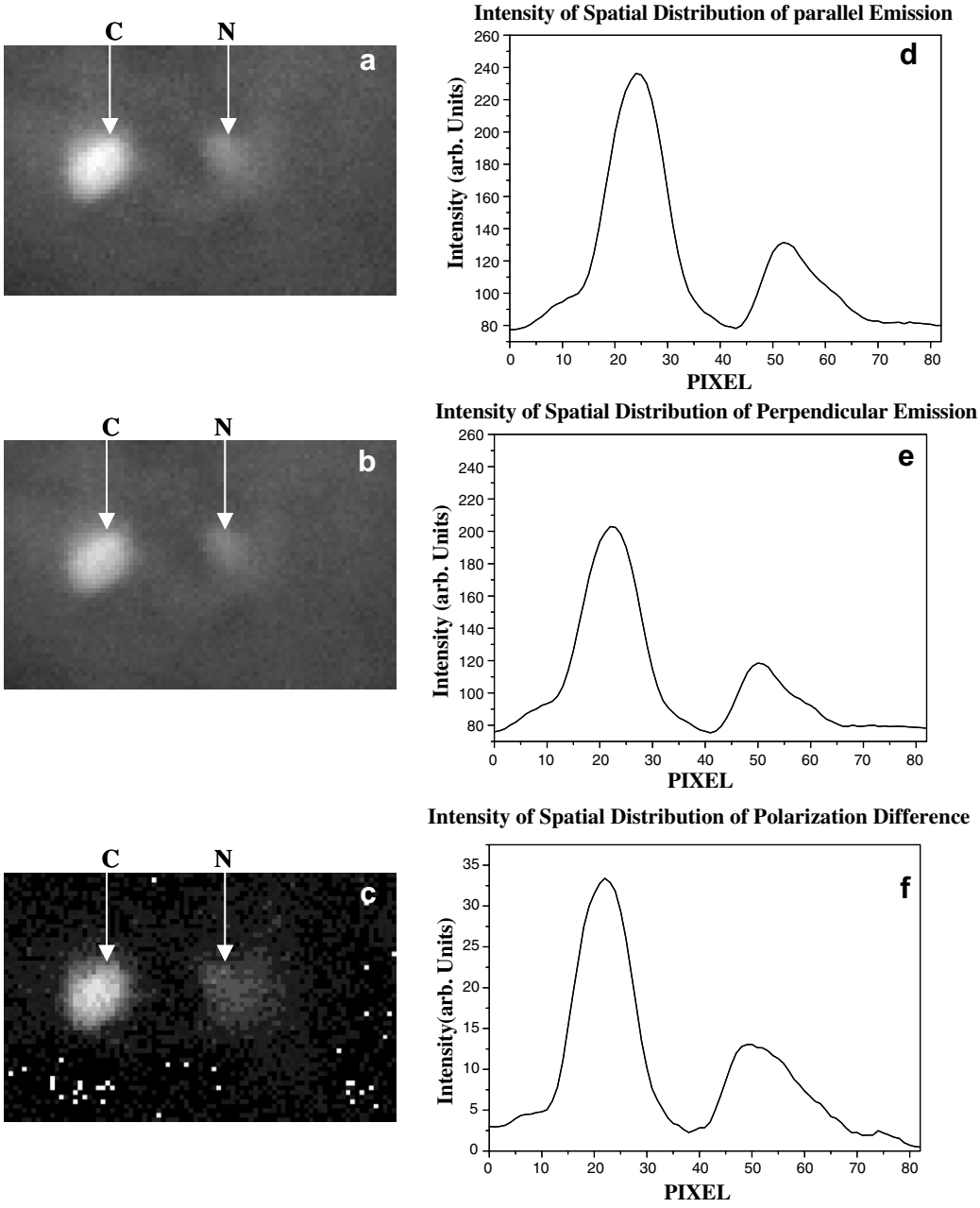

Fig. 5. Polarization dependence of the contrast agent emission images of a cancerous-and-normal prostate tissue sample (a Cybesin-stained tiny cancerous prostate tissue piece and a Cybesin-stained tiny normal prostate tissue piece sandwiched by large pieces of normal prostate tissue) recorded at $\lambda_{pump} = 750$ nm and $\lambda_{detection} = 850$ nm when the polarization direction of P_2 is parallel (a) and perpendicular (b) to that of the illuminating light. Panel (c) is the polarization difference image obtained by subtracting (b) from (a). Panels (d)–(f) are the digital spatial cross-section intensity distributions of the images shown in (a)–(c) at a row crossing the areas of the stained cancer (C) and normal (N) tissues, respectively.

In addition, the improvement of the spatial resolution of the difference image in comparison with the individual polarization images can be seen from Fig. 5d–f. The full-width at half-maximum (FWHM) for the cancerous tissue area shown in Fig. 5f is improved by a factor of 1.36 with respect to that of the conventional image. The improvement of the spatial resolution of the difference image can be understood because the fluorescence polarization difference image cancelled out the strong diffusive component of the emission and only kept the contribution from ballistic photons and partial snake photons [12]. The enhancement of contrast between the cancerous and the normal areas is due to the higher polarization anisotropy of Cybesin contained in cancerous tissue. Since the difference of $I_{\parallel} - I_{\perp}$ for the Cybesin-stained cancerous tissue is larger than that in the Cybsein-stained normal tissue, the contrast between cancerous and normal tissue areas is improved.

5. Conclusion

Time-resolved fluorescence kinetics and polarization anisotropy of a receptor-targeted contrast agent, Cybesin, in solution and in stained human cancerous and normal prostate tissues were measured. The experimental results indicate that Cybesin solutions and Cybesin-stained prostate tissue have the polarization preservation property. The fluorescence intensity emitted from a Cybesin-stained cancerous tissue area was found to be much stronger than that from a Cybesin-stained normal tissue area indicating that cancerous prostate tissue takes-up more Cybesin than normal tissue. This property makes Cybesin a potential marker for prostate cancer. The experimental data obtained from a Cybesin solution was fitted using a time-dependent fluorescence depolarization model. An empirical model was developed to describe the time-resolved fluorescence kinetics and polarization anisotropy of Cybesin in stained prostate tissue. A static anisotropy component formed by the emission of prostate cell-bonded Cybesin molecules (without rotation), and a time-dependent anisotropy component formed by the emission of unbonded Cybesin molecules (with rotation) were determined. The anisotropy value of Cybesin in stained cancerous tissue was found to be much higher than that in stained normal tissue indicating a larger polarization preservation property of Cybesin in stained cancerous tissue than in stained normal tissue. Optical imaging of cancerous and normal prostate tissue stained with Cybesin was investigated. The fluorescent image of Cybesin-stained cancerous prostate tissue was found to be much brighter than that of Cybesin-stained normal tissue. The fluorescence-polarization-difference-imaging technique was used to enhance the contrast between cancerous and normal tissue areas.

For application of this research, both time-resolved polarization-dependent fluorescence of Cybesin in prostate tissue and fluorescence polarization difference imaging may be used to enhance the contrast between cancerous and normal prostate tissues, and distinguish prostate cancerous tissue from the normal in biopsy sample analysis in addition to histological results. The imaging experiments indicate that the NIR imaging of prostate tissue enhanced by Cybesin is a potential approach for screening, monitoring and identifying the cancerous prostate tissue from the surrounding normal tissue. This work may introduce a new criteria/indicator for prostate cancer screening in addition to the conventional PSA blood test, a DRE and TRUS examination.

6. Future work

The immunochemical analysis is needed to confirm and study the bombesin receptors in collaboration with immunochemistry experts. The optical imaging and immunochemistry measurements need to be performed and compared for various cancerous prostate tissue samples with different types and Gleason grades of cancers [22] as well as control normal prostate tissue samples to investigate the presence of the bombesin receptor and the uptaking of the Cybesin as a function of types and Gleason grades of prostate cancers.

Acknowledgements

This research is supported by a US Army Medical Research and Material Command Grant No. DAMD17-01-1-0084 (CUNY RF 47462-00-01). The authors acknowledge useful comments from Dr. N. Ockman, the help of NDRI, CHTN and HUMC for providing normal and cancer prostate tissue samples, and the help of Mr. M. Jeanty at IUSL in the time-resolved fluorescence measurements.

References

[1] D.J. Tindall, P.T. Scardino, Prostate 38 (2) (1999) 166.
[2] D.D. Shaw, Invest. Radiol. 28 (1993) 110.
[3] R.R. Alfano, D. Tata, J. Cordero, P. Tomashefsky, F. Longo, M. Alfano, IEEE J. Quantum Electron. 20 (1984) 1507.
[4] David A. Benaron, Cancer Metast. Rev. 21 (2002) 45.
[5] Kendric C. Smith, The Science of Photobiology, second ed., Plenum Press, New York, 1989.
[6] Donna J. Dean, Brenda J. Korte, Opt. Photon. News (2003). Available from: <http://ultra.bu.edu/papers/2003_10_OPN.pdf>.
[7] M.A. Clause, R.K. Jain, Cancer Res. 50 (1990) 3487.
[8] D.J. Bornhop, C.H. Contag, K. Licha, C.J. Murphy, J. Biomed. Opt. 6 (2001) 106.
[9] J.E. Bugaj, S. Achilefu, R.B. Dorshow, R. Rajagopalan, J. Biomed. Opt. 6 (2) (2001) 122.
[10] Jean Claude Reubi, Sandra Wenger, Jacqueline Schmuckli-Maurer, Jean-Claude Schaer, Mathias Gugger, Clin. Cancer Res. 8 (2002) 1139.
[11] Y. Pu, W.B. Wang, G.C. Tang, F. Zeng, S. Achilefu, J.H. Vitenson, I. Sawczuk, S. Peters, J.M. Lombardo, R.R. Alfano, Technol. Cancer Res. Treat. 4 (2005) 429.
[12] W.B. Wang, S.G. Demos, J. Ali, R.R. Alfano, Opt. Commun. 142 (1997) 161.
[13] Wubao Wang, Jamal H. Ali, R.R. Alfano, J.H. Vitenson, J.M. Lombardo, IEEE J. Select. Top. Quantum Electron. 9 (2003) 288.
[14] G.R. Fleming, J.M. Morris, G.W. Robinson, Chem. Phys. 17 (1976) 91.
[15] G. Porter, P.J. Sadkowski, C.J. Tredwell, Chem. Phys. Lett. 49 (1977) 416.
[16] A. Szabo, J. Chem. Phys. 72 (8) (1980) 4620.
[17] F. Pellegrino, A dissertation thesis of the City University of New York, 1981, p. 270 (Chapter 9).
[18] F. Pellegrino, P. Sekuler, R.R. Alfano, Photobiochem. Photobiophys. 2 (1981) 15.
[19] D.A. Beysens, G. Forgacs, J.A. Glazier, Proc. Natl. Acad. Sci. USA 97 (2000) 9467.
[20] Jean Paul Rieu1, Yasuji Sawada, Eur. Phys. J. B 27 (2002) 167.
[21] M.A. Dresner, P.J. Rossman, S.A. Kruse, R.L. Ehman, "MR Elastography of the Prostate", ISMRM 99 CDs. Available from: <http://cds.ismrm.org/ismrm-1999/PDF2/526.pdf>.
[22] Prostate Cancer Foundation, "Gleason Grade – Prostate Cancer Overview". Available from: <http://www.prostatecancerfoundation.org/site/c.itIWK2OSG/b.47290/k.FC08/Screening_Diagnosis_and_the_Gleason_Grade.htm>.